

Evaluation of antibacterial and cytocompatible properties of multiple-ion releasing zinc-fluoride glass nanoparticles

Erika NISHIDA¹, Hirofumi MIYAJI¹, Kanako SHITOMI¹, Tsutomu SUGAYA¹ and Tsukasa AKASAKA²

¹ Department of Periodontology and Endodontology, Faculty of Dental Medicine, Hokkaido University, N13 W 7, Kita-ku, Sapporo, Hokkaido 060-8586, Japan

² Department of Biomedical Materials and Engineering, Faculty of Dental Medicine, Hokkaido University, N13 W 7, Kita-ku, Sapporo, Hokkaido 060-8586, Japan

Corresponding author, Hirofumi MIYAJI; E-mail: miyaji@den.hokudai.ac.jp

Zinc-fluoride glass nanoparticles (Zinc-F) release several ions, such as fluoride, zinc and calcium ions, through acid-base reactions. The aim of this study was to evaluate the antibacterial and cytotoxic properties of Zinc-F. Antibacterial tests showed that a Zinc-F eluting solution significantly reduced the turbidity and colony-forming units of *Streptococcus mutans* and *Actinomyces naeslundii*, compared to that of calcium-fluoroaluminosilicate glass nanoparticles without zinc ions. In live/dead staining, Zinc-F eluate significantly decreased green-stained bacterial cells, indicating live cells, compared with the control (no application). Human dentin coated with Zinc-F showed suppressed *S. mutans* and *A. naeslundii* biofilm formation. Additionally, Zinc-F eluate showed low cytotoxic effects in osteoblastic and fibroblastic cells. Therefore, our findings suggested that Zinc-F exhibits antibacterial and biocompatible properties through multiple-ion release.

Keywords: *Actinomyces naeslundii*, Biocompatibility, Dentin, *Streptococcus mutans*, Zinc-fluoride glass nanoparticles

INTRODUCTION

Root caries has become a major problem in elderly people with exposed tooth roots caused by aging or periodontal disease. In severe cases of root caries, the damaged tooth is extracted, consequently reducing oral function¹. Very elderly people need non-invasive approaches to safely treat root caries, instead of classical restorative therapies such as glass ionomer or composite resin filling with local anesthesia. Hence, easy handling and effective dental materials are required to attack the bacterial biofilm, stop caries progression and achieve root remineralization.

Multifunctional bioactive nanomaterials are used for root surface modification as drug delivery systems. Nano-sized substances tend to have high bioactivity at the biointerface because of their high surface area to volume ratio. Eshed *et al.* reported that tooth surface modification using magnesium-fluoride nanoparticles effectively prevents *Streptococcus mutans* biofilm formation². Examination using human dentin showed that the application of fluoride-containing aluminocalciumsilicate nanoparticles exerted resistance against dentin demineralization in acid solution^{3,4}. In addition, calcium and silica were incorporated into the dentin surface from applied nanoparticles to modify the dentin surface^{3,4}. Thus, nanomodification of the root surface using antibacterial and/or remineralizing materials is anticipated as a novel root caries therapy.

Recently, the nanoparticulate glass product CAREDYNE™ SHIELD (GC, Tokyo, Japan) was launched for dental treatment of hypersensitivity. It is composed of two liquids, an aqueous dispersion of zinc-fluoride glass nanoparticles (Zinc-F) containing zinc, fluoride,

calcium and silicon and a phosphoric acid solution. It is assumed that Zinc-F aggregates on the dentin surface to close dentinal tubules and release zinc, fluoride, calcium and silicon ions through acid-base reactions, such as silicate cement⁵, after mixing with phosphoric acid. Zinc-related substances are well-known to contribute to antibacterial activity. For instance, ZnO damages the bacterial cell membrane, resulting in intracellular matrix leakage and bacterial cell death⁶. Zinc possesses a catalytic effect to generate reactive oxygen species^{7,8}. Furthermore, zinc ions reduce acid production of *S. mutans*⁹ and prevent collagen degradation to suppress the progression of tooth decay^{10,11}. Furthermore, fluoride ions typically show tooth remineralizing and antibacterial effects. Featherstone *et al.* showed that fluoride-incorporated apatite significantly improved inhibition of *S. mutans* growth and dissolution of calcium phosphate in a citric acid buffer when compared with an apatite-only sample^{12,13}. Accordingly, we considered that application and tooth modification using Zinc-F would prevent root caries formation and progression through the release of zinc and fluoride ions.

In this study, we examined the antibacterial activity of Zinc-F. An eluting solution of acidized Zinc-F was evaluated in antibacterial assessments using a dental caries pathogen, *S. mutans*, and a primary colonizer of biofilms, *Actinomyces naeslundii*¹⁴. In addition, we assessed the antibacterial effect of Zinc-F application on human dentin blocks. Because antibacterial biomaterials frequently exhibit cytotoxicity, the cytocompatibility of Zinc-F in mammalian cells was also investigated.

MATERIALS AND METHODS

Fabrication of eluting solution and ion release test

A dispersion of Zinc-F (median diameter: 300–500 nm; GC) was used in all experiments. As a control, a dispersion of calcium-fluoroaluminosilicate glass nanoparticles (NS) in a product for dental treatment of hypersensitivity (Nanoseal[®], Nippon Shika Yakuhin, Shimonoeki, Japan) was used. The dispersion of Zinc-F or NS was mixed with 12% phosphoric acid for 5 s in a weight ratio of 1:1. After removing the phosphoric acid, the mixture was dried and dispersed in distilled water to obtain a 3 wt% aqueous dispersion. This dispersion was stirred for 1, 4, 7, 14, 21 and 28 days using a magnetic stirrer and was then centrifuged (4,000 rpm, 2 min) to obtain eluting solutions. The fluoride ion volume in the solution was measured using a fluoride ion meter (LAQUA F-72, Ion electrode 6583, HORIBA, Kyoto, Japan). The zinc and calcium ion volumes were measured using inductively coupled plasma atomic emission spectroscopy (iCAP 7200 Duo, Thermo Fisher Scientific, Waltham, MA, USA).

Antibacterial effects of Zinc-F and NS eluting solution

S. mutans ATCC 35668 and *A. naeslundii* ATCC 27039 were obtained from the American Type Culture Collection (Manassas, VA, USA) and kept frozen until analysis. Brain heart infusion (BHI) broth (Pearlcore[®], Eiken Chemical, Tokyo, Japan) containing 0.1% antibiotic (0.05% gramicidin D and 0.05% bacitracin, FUJIFILM Wako Pure Chemical, Osaka, Japan) with 1% sucrose (FUJIFILM Wako Pure Chemical) and *Actinomyces* broth (BBL[™] *Actinomyces* Broth, Becton, Dickinson and Company, Franklin Lakes, NJ, USA) were selected as culture media for *S. mutans* and *A. naeslundii*, respectively.

For turbidity assays, a Zinc-F and NS eluting solution (stirred for 1 day) was added to suspensions of *S. mutans* (final concentration: 7.3×10^6 colony-forming unit (CFU)/mL) and *A. naeslundii* ATCC (final concentration: 2.3×10^6 CFU/mL). The Zinc-F or NS eluate concentration (2 or 20 wt%) was decided based on findings from a previous study¹⁵. The concentration was adjusted by adding a phosphate-buffered solution (PBS, FUJIFILM Wako Pure Chemical) as follows. To make a 20 wt% elute, 20% eluting solution was mixed with 80% suspension; to make a 2 wt% elute, 2% eluting solution was mixed with 18% PBS and 80% suspension. The control contained 20% PBS and 80% suspension only. Subsequently, the bacterial suspension was dispensed into wells of 48-well plates and cultured for 24 h at 37°C under anaerobic conditions. After incubation, the suspension was ultrasonically homogenized and then bacterial turbidity was measured using a colorimeter (CO7500 Colourwave, Funakoshi, Tokyo, Japan) at an absorbance of 590 nm. In addition, cultured suspensions including Zinc-F or NS eluate (20 wt%) were ultrasonically homogenized, diluted in medium, and spread onto BHI agar plates (Pearlcore[®], Eiken Chemical). After anaerobic incubation at 37°C for 24 h, CFUs were determined.

Three incubated samples applied with Zinc-F eluting solution were stained using the LIVE/DEAD BacLight Bacterial Viability Kit (Thermo Fisher Scientific) and observed using a fluorescence microscope (BioRevo BZ-9000, Keyence, Osaka, Japan). Live bacteria were stained with SYTO9 to create green fluorescence, and bacteria with compromised membranes were stained with propidium iodide to create red fluorescence. The fluorescence intensity was measured using software (ImageJ 1.41, National Institutes of Health, Bethesda, MD, USA) to calculate the percentage of live and dead cells.

Morphological analysis of Zinc-F-coated human dentin blocks

Human vital third molars, which were extracted in standard dental treatments, were cut to obtain dentin blocks (5×5×1 mm) using a diamond disc (Horico diamond disc 87xFSI, Horico, Berlin, Germany). Thereafter, dentin blocks were polished with sandpaper (#600 and #2000) and treated with 3% ethylenediaminetetraacetic acid (Smear Clean, Nippon Shika Yakuhin) for 4 min to remove the smear layer. After ultrasonic cleaning, dentin blocks were sterilized by UV light for 24 h and were then obtained for investigation. The use of human teeth in this study was approved by the Institutional Review Board of Hokkaido University Hospital for Clinical Research (approval no. 17-222).

Subsequently, dentin blocks were immersed in a mixture of Zinc-F dispersion and 12% phosphoric acid at a weight ratio of 1:1 for 20 s and then washed with PBS. As a control, dentin blocks not coated with Zinc-F were used. After ethanol dehydration, drying and Pt-Pd coating, the dentin block surface was characterized by field emission scanning electron microscopy (SEM) in conjunction with energy dispersive X-ray (EDX) spectrometry (JSM-6500F, JEOL, Tokyo, Japan).

Antibacterial assessment of Zinc-F-coated human dentin blocks

In order to simulate clinical settings, the antibacterial activity of Zinc-F-coated dentin was investigated. Dentin blocks coated with Zinc-F were placed at the bottom of wells in a 48-well plate. Suspensions of *S. mutans* (final concentration: 2.8×10^6 CFU/mL) and *A. naeslundii* (final concentration: 1.1×10^7 CFU/mL) were then seeded onto the Zinc-F-coated dentin and anaerobically cultured for 24 h. As a control, dentin blocks coated with PBS only were used. For morphological observations of *S. mutans* and *A. naeslundii*, inoculated samples were fixed in 2.5% glutaraldehyde in a 0.1 M sodium cacodylate buffer (pH 7.4) and then dehydrated in increasing concentrations of ethanol. After critical point drying and Pt-Pd coating, samples were analyzed using SEM (S-4000, Hitachi, Tokyo, Japan) at an accelerating voltage of 10 kV. The exposed dentin area was measured from SEM images using ImageJ 1.41.

Cytotoxic assessment of Zinc-F eluting solution

To evaluate the cytotoxicity of Zinc-F, an eluting

solution (0, 2 or 20 wt%) was added to a suspension of 1×10^4 mouse osteoblastic MC3T3-E1 cells (RIKEN BioResource Center, Tsukuba, Japan) and fibroblastic NIH3T3 cells (RIKEN BioResource Center) cultured in 48-well plates. Cultures were then incubated at 37°C with 5% CO₂ using culture medium (minimum essential medium alpha, GlutaMAX-I, Thermo Fisher Scientific) supplemented with 10% fetal bovine serum (Qualified FBS, Thermo Fisher Scientific) and 1% antibiotics (penicillin-streptomycin, Thermo Fisher Scientific). The concentration of culture medium was adjusted by adding PBS, similarly to antibacterial assessments. Cytotoxicity after incubation for 1 and 3 days was determined using the water-soluble tetrazolium salt-8 (WST-8) assay (Cell Counting Kit-8, Dojindo Laboratories, Mashiki, Japan). Absorbance at 450 nm was measured using a microplate reader (Multiskan FC, Thermo Fisher Scientific).

In addition, some samples were stained using the LIVE/DEAD Viability/Cytotoxicity Kit for mammalian cells (Thermo Fisher Scientific), following the manufacturer's instructions. Live cells were stained with calcein acetoxymethyl to create green fluorescence, and cells with compromised membranes were stained with ethidium homodimer-1 to create red fluorescence. Stained samples were examined using fluorescence microscopy. Fluorescence intensity was measured using ImageJ 1.41.

Statistical analysis

Means and standard deviations of each parameter were calculated. Differences between the groups were analyzed using Scheffé's method and Mann-Whitney *U* test. *p*-Values <0.05 were considered to be statistically significant. All statistical procedures were performed using SPSS 11.0 (IBM Corporation, Armonk, NY, USA).

RESULTS

Ion release profile of Zinc-F

The amounts of released ions from acidized Zinc-F and NS are shown in Fig. 1. The Zinc-F eluting solution contained fluoride, zinc and calcium ions. The release of these three ions rapidly increased until 7 days, and proceeded gradually through the experimental period. NS eluting solution contained fluoride and calcium ions, but not zinc ions. The release of ions rapidly increased until 7 days; however, the amounts of fluoride and calcium ion were consistently low when compared to Zinc-F.

Antibacterial activity of Zinc-F

The results of turbidity measurements are shown in Fig. 2A. Turbidity of the control (no application), low-dose Zinc-F eluting solution (2 wt%), high-dose Zinc-F eluting solution (20 wt%), low-dose NS eluting solution (2 wt%) and high-dose NS eluting solution (20 wt%) are 0.23, 0.17, 0.04, 0.25 and 0.24, respectively. The application of 20 wt% Zinc-F eluting solution significantly decreased the turbidity of *S. mutans* when compared with 2 wt% Zinc-F eluting solution and the control (no application) ($p < 0.01$). In addition, 20 wt% Zinc-F eluting solution significantly reduced the turbidity when compared with 2 and 20 wt% NS eluting solution ($p < 0.01$). In CFU assessments, 20 wt% Zinc-F eluting solution significantly reduced the bacterial concentration for *S. mutans* ($p < 0.01$) and *A. naeslundii* ($p < 0.05$) when compared with NS eluting solution (Fig. 2B).

From the results of live/dead staining, the 20 wt% Zinc-F eluting solution increased the intensity of red-stained *S. mutans* and *A. naeslundii* cells related to dead bacteria, and decreased the intensity of green-stained cells indicating viable bacteria (Fig. 3A). Software based quantification revealed that green and red intensity

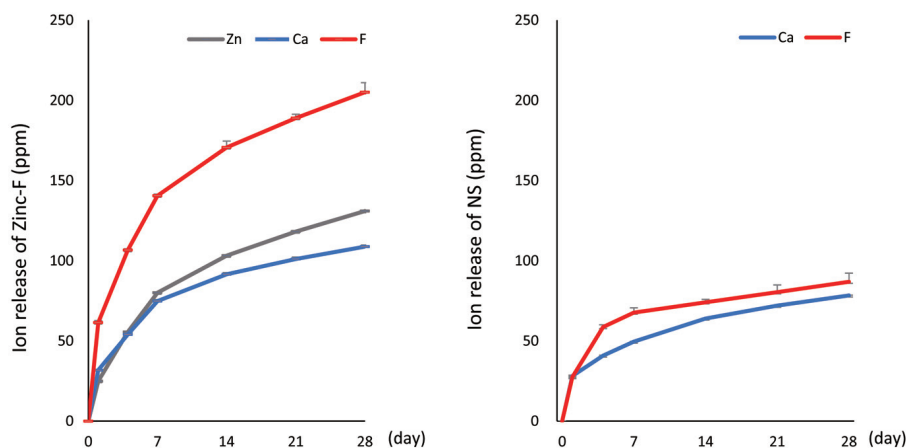


Fig. 1 Ion release profiles for zinc, calcium and fluoride ions from Zinc-F and NS ($n=3$, mean \pm SD). NS, calcium-fluoroaluminosilicate glass nanoparticles; SD, standard deviation; Zinc-F, zinc-fluoride glass nanoparticles.

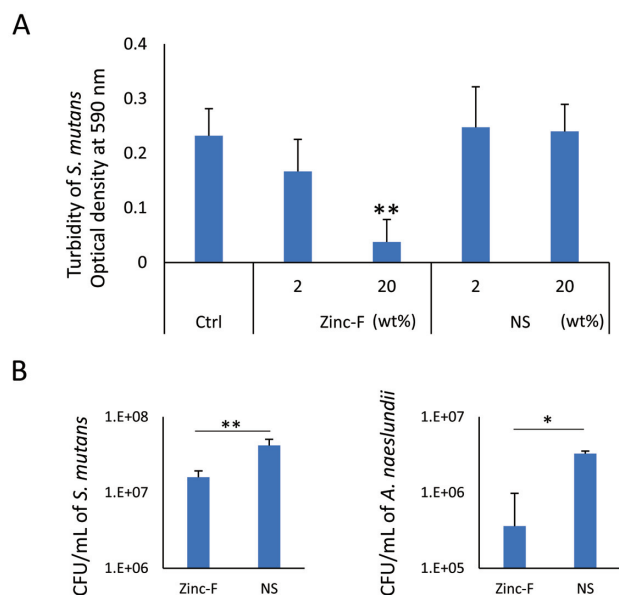


Fig. 2 Turbidity assessments. (A) Turbidity for *S. mutans* and *A. naeslundii* after 24-h incubation with 0 (control), 2 or 20 wt% Zinc-F eluate and 2 or 20 wt% NS elute ($n=6$, mean \pm SD). ** $p<0.01$, vs. all other groups. (B) Number of CFU/mL of *S. mutans* and *A. naeslundii* after 24-h incubation with 20 wt% Zinc-F or NS eluate ($n=5$, mean \pm SD). * $p<0.05$, ** $p<0.01$. CFU, colony-forming unit; NS, calcium-fluoroaluminosilicate glass nanoparticles; SD, standard deviation; Zinc-F, zinc-fluoride glass nanoparticles.

($10^4 \times \text{pixel}$) of 0, 2 and 20 wt% Zinc-F eluting solution was 89.6 and 0.9, 87.4 and 4.6, 41.6 and 8.1 in *S. mutans* and 105.5 and 0.6, 87.3 and 3.6, 73.1 and 4.5 in *A. naeslundii*, respectively. The live cell (%) of 0, 2 and 20 wt% Zinc-F eluting solution was 99.0, 95.0, 83.7 in *S. mutans* and 99.4, 96.1, 94.2 in *A. naeslundii*, respectively. The 20 wt% Zinc-F eluting solution significantly reduced the intensity of green fluorescence from *S. mutans* and *A. naeslundii* cells compared with the 2 wt% Zinc-F eluting solution and the control ($p<0.05$). In addition, the fluorescence intensity for *A. naeslundii* treated with the 2 wt% Zinc-F eluting solution was significantly lower than that for the control ($p<0.05$). Application of Zinc-F eluting solution significantly increased the intensity of red fluorescence for *S. mutans* ($p<0.05$) and *A. naeslundii* ($p<0.01$) compared with that for the control. In addition, the intensity of red fluorescence for *S. mutans* treated with the 20 wt% Zinc-F eluting solution was significantly increased when compared with that for the 2 wt% Zinc-F eluting solution ($p<0.05$) (Fig. 3B).

Morphological analysis of Zinc-F-coated human dentin blocks

SEM and EDX assessments are shown in Fig. 4. SEM images of the dentin surface showed that numerous aggregated nanoparticles were present on dentin

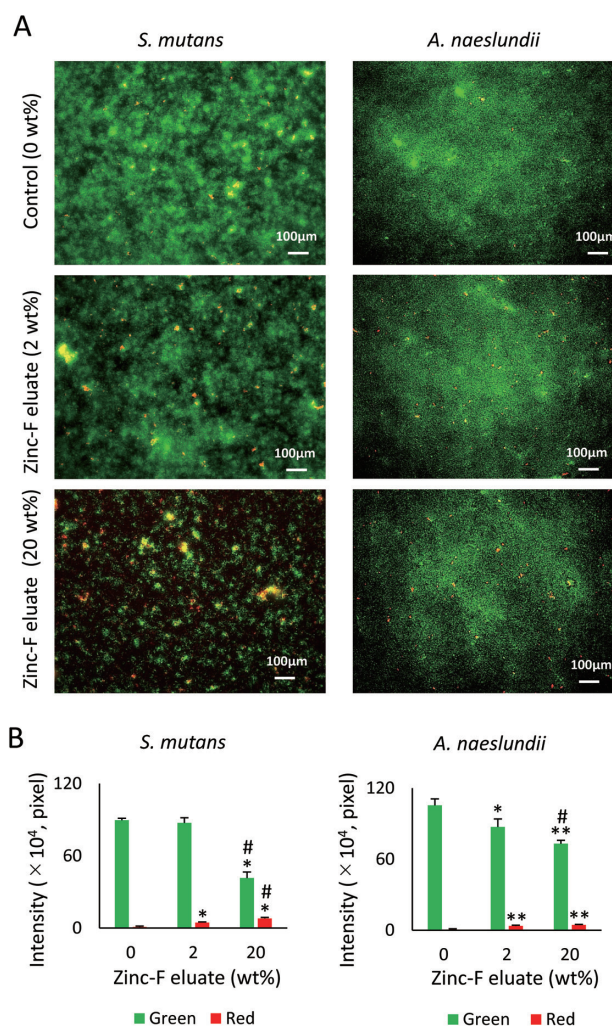


Fig. 3 LIVE/DEAD BacLight staining for antibacterial properties. (A) LIVE/DEAD BacLight staining of *S. mutans* and *A. naeslundii* after 24-h incubation receiving 0 (control), 2 or 20 wt% Zinc-F eluate. (B) Fluorescence intensity for live (green) and dead (red) cells ($n=3$, mean \pm SD). * $p<0.05$ and ** $p<0.01$, vs. 0 wt% Zinc-F eluate; # $p<0.05$, vs. 2 wt% Zinc-F eluate. SD, standard deviation; Zinc-F, zinc-fluoride glass nanoparticles.

coated with Zinc-F when compared with the control. Nanoparticles frequently invaded open dentinal tubules on the dentin surface. EDX analysis revealed that C, P and Ca from the dentin substrate were present in both samples. Si related to Zinc-F was only detected on Zinc-F-coated dentin.

Antibacterial evaluation of dentin blocks coated with Zinc-F

SEM images after *S. mutans* and *A. naeslundii* seeding on dentin are shown in Figs. 5A and B. Biofilm formation of *S. mutans* and *A. naeslundii* was frequently observed on the dentin of the control group (no application).

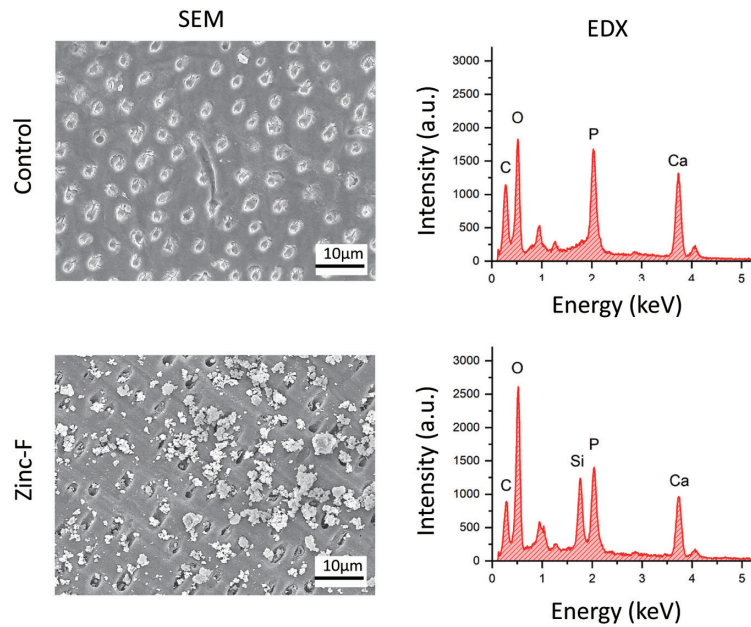


Fig. 4 Characterization of dentin coated with Zinc-F. SEM micrographs and EDX analysis of human dentin in control (no application) and Zinc-F-coated groups. EDX, energy dispersive X-ray spectrometry; SEM, scanning electron microscopy; Zinc-F, zinc-fluoride glass nanoparticles.

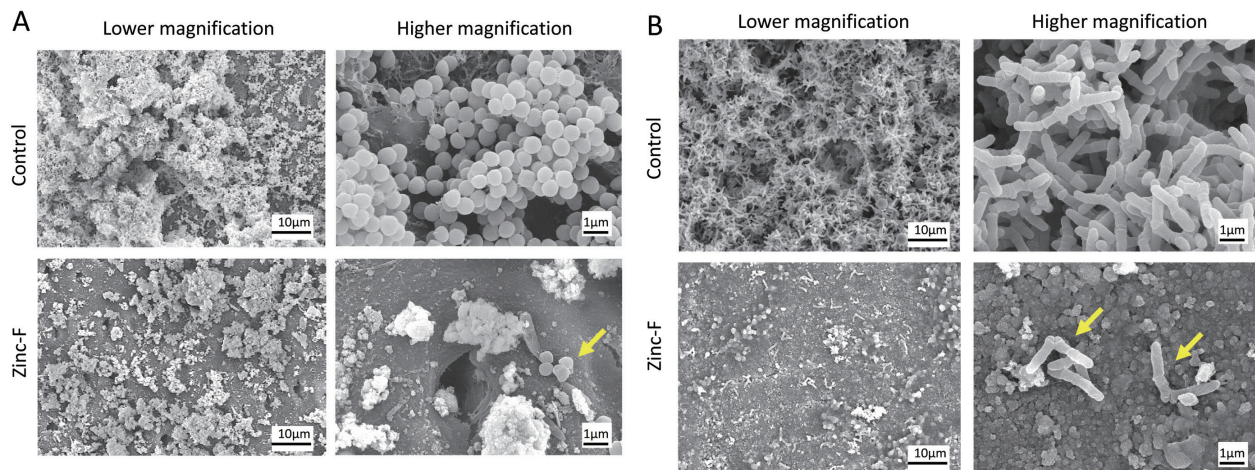


Fig. 5 Antibacterial effect of dentin coated with Zinc-F. Low- and high-magnification of SEM images of human dentin after *S. mutans* (A) and *A. naeslundii* (B) seeding and 24-h incubation in control (no application) and Zinc-F-coated groups. Arrow indicates atrophic-shaped *S. mutans* and *A. naeslundii* cells. Zinc-F, zinc-fluoride glass nanoparticles.

Biofilms were layered and widely covered the dentin surface. In contrast, the Zinc-F-coated group rarely demonstrated *S. mutans* and *A. naeslundii* biofilm formation. Although bacterial cells clustered slightly around aggregated nanoparticles, the cell shape was frequently atrophied (yellow arrows). The rate of exposed dentin area in control and Zinc-F-coated dentin was 36.3 and 66.5% in *S. mutans* and 23.7 and 82.6% in *A. naeslundii*, respectively. Control specimens

were significantly lower than those of Zinc-F-coated specimens ($p < 0.05$) (Fig. 6).

Cytotoxic assessment of Zinc-F

In order to assess the cytocompatibility of Zinc-F, WST-8 activity of fibroblastic and osteoblastic cells was measured (Fig. 7). All groups showed increased WST-8 activity from 1 day to 3 days. There were no significant differences between any group ($p > 0.05$). Live/dead

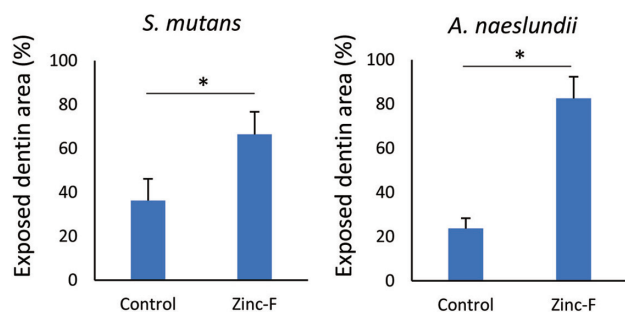


Fig. 6 Exposed dentin area assessments. Exposed dentin area after *S. mutans* and *A. naeslundii* seeding ($n=4$, mean \pm SD). * $p<0.05$. SD, standard deviation; Zinc-F, zinc-fluoride glass nanoparticles.

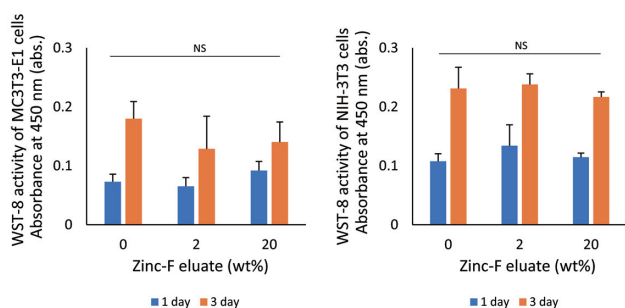


Fig. 7 WST-8 activity assessment. WST-8 activity for MC3T3-E1 cells and NIH3T3 cells at 1 and 3 days ($n=4$, mean \pm SD). NS, not significant; SD, standard deviation; WST, water-soluble tetrazolium salt; Zinc-F, zinc-fluoride glass nanoparticles.

staining revealed that cells treated with Zinc-F eluting solution were mostly stained in green, indicating live cells (Fig. 8). All groups showed equivalent intensity of fluorescence ($p>0.05$) (Fig. 7B).

DISCUSSION

Assessment of the ion release profile showed that acidized Zinc-F could continuously release multiple ions, including zinc, fluoride and calcium ions. In addition, 20 wt% eluting solution of acidized Zinc-F, including large quantities of fluoride ions, consistently reduced the CFU of oral bacteria *S. mutans* and *A. naeslundii* compared with eluting solution of NS, and decreased the number of bacterial cells stained in green, indicating live cells, in live/dead staining examination. Hence, we considered that Zinc-F is capable of growth inhibition of oral bacteria by releasing multiple and large quantities of ions. It is difficult to reproduce *in vivo* oral saliva flow conditions. When clinically applying CAREDYNE™ SHIELD following the manufacturer's instructions, the amount of Zinc-F applied to the tooth is 0.02 g. An

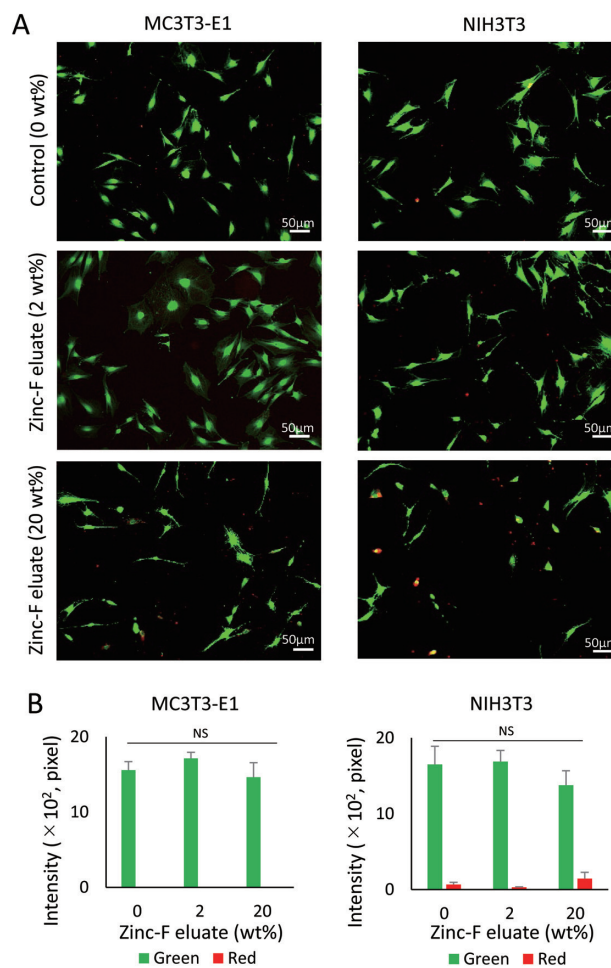


Fig. 8 LIVE/DEAD BacLight staining for cytotoxic properties.

(A) LIVE/DEAD BacLight staining of MC3T3-E1 cells and NIH3T3 cells after 24-h incubation receiving 0 (control), 2 or 20 wt% Zinc-F eluate. (B) Fluorescence intensity of live (green) and dead (red) cells ($n=4$, mean \pm SD). NS, not significant; SD, standard deviation; Zinc-F, zinc-fluoride glass nanoparticles.

eluting solution of 20 wt% is theoretically obtained from 0.02 g Zinc-F and 3 mL water. It has been reported that unstimulated salivary flow rate is 0.3–0.4 mL/min¹⁶. Accordingly, we considered that the 20% eluting solution used in this assessment had a relatively low ion concentration when compared to CAREDYNE™ SHIELD application in clinical settings, and is thus expected to further antibacterial activity of Zinc-F in dental treatment.

Reportedly, fluoride application enhances the accumulation of protons in cells to reduce the tolerance of bacteria under acidic conditions^{17,18}. In addition, fluoride affects the metalloenzyme, enolase, to downregulate the glycolytic pathway¹⁹. Hence, Zinc-F likely exerted the growth-inhibitory effects on oral bacterial cells through

fluoride ion release. However, a higher fluoride ion concentration would be needed to kill bacterial cells. Nassar and Gregory revealed that *S. mutans* strains were not able to form biofilms at fluoride concentrations >225 ppm (in contrast to ≤62 ppm applied in this study)²⁰. Thus, we presume that the bactericidal activity of Zinc-F is related to the synergistic effects of zinc and fluoride ions. Phan *et al.* demonstrated that zinc ions exhibit antibacterial effects against *S. mutans* through inhibition of glycolysis, the sugar phosphotransferase system and F-adenosine triphosphate; however, these inhibitory effects are reversible²¹. They considered that zinc ions mostly exhibited a bacteriostatic effect. Izaguirre-Fernández *et al.* demonstrated that zinc alone showed slight effects on viability of *S. mutans*; however, application of zinc and fluoride enhanced the antimetabolic activity of fluoride to consequently promote bactericidal effects²². Accordingly, Zinc-F likely promotes antibacterial activity through release of both fluoride and zinc ions, even at low concentrations. Further study is required to fully elucidate the mechanisms involved.

Clinically, fluoride application has been attempted to prevent root caries. Fluoride toothpaste, varnish and mouthwash demonstrated a caries-preventive effect²³⁻²⁵. Hence, application of Zinc-F may strengthen the tooth by releasing fluoride ions. In addition, the tooth protecting activity of zinc has been reported. Takatsuka *et al.* revealed that zinc and fluoride-containing toothpaste suppressed dentin demineralization when compared with zinc-free fluoride toothpaste²⁶. Concerning the mechanism underlying the inhibitory activity of zinc, it is considered that the cationic effect of zinc stimulates binding between collagen and other matrix proteins to resist biodegradation. Osorio *et al.* demonstrated that artificial saliva including zinc reduces human dentin collagen degradation related to matrix metalloproteinases-2²⁷. Zinc-F seems to provide multiple beneficial effects for prevention of root caries.

SEM and EDX analyses showed that Zinc-F aggregation could remain on the human dentin surface after washing with PBS, and so inhibit *S. mutans* and *A. naeslundii* growth. It was considered that the attached Zinc-F releases multiple ions to exhibit its antibacterial effect. We considered that the multiple ions released from acidized Zinc-F and the decalcified tooth surface react with each other to form precipitates, such as $Zn_3(PO_4)_2$ and $Ca_3(PO_4)_2$, to bind Zinc-F on the dentin surface, as in the case of aluminosilicate glass²⁸. From the evidence of long-term ion release, tooth surface modification using Zinc-F likely exerts a plaque-reducing effect and promotes oral health. In addition, Zinc-F showed low cytotoxic effects in the WST-8 assay and live/dead staining investigation. Recently, silver diamine fluoride has been applied to inhibit tooth caries progression²⁹. However, silver diamine fluoride reportedly exhibits high cytotoxicity and blackens teeth. The biocompatible characteristics of Zinc-F offer advantages for clinical applications to oral tissue.

CONCLUSION

We herein assessed the antibacterial and cytotoxic effects of Zinc-F. Acidized Zinc-F released multiple ions such as fluoride, zinc and calcium ions. Zinc-F showed inhibitory effects against *S. mutans* and *A. naeslundii* but had low cytotoxicity in mammalian cells. In addition, Zinc-F exhibited antibacterial effects after application to human dentin. Thus, Zinc-F is promising for prevention and treatment of oral diseases, especially root caries.

CONFLICT OF INTEREST

The authors report that they have no conflict of interest related to this study.

REFERENCES

- Wyatt CC, MacEntee MI. Dental caries in chronically disabled elders. *Spec Care Dentist* 1997; 17: 196-202.
- Eshed M, Lellouche J, Banin E, Gedanken A. MgF₂ nanoparticle-coated teeth inhibit *Streptococcus mutans* biofilm formation on a tooth model. *J Mater Chem B* 2013; 1: 3985-3991.
- Han L, Okiji T. Effects of a novel fluoride-containing aluminocalciumsilicate-based tooth coating material (Nanoseal) on enamel and dentin. *Am J Dent* 2013; 26:191-195.
- Miyajima H, Ishimoto T, Ma S, Chen J, Nakano T, Imazato S. In vitro assessment of a calcium-fluoroaluminosilicate glass-based desensitizer for the prevention of root surface demineralization. *Dent Mater J* 2016; 35: 399-407.
- Wilson AD, Batchelor RF. Dental silicate cements. I. The chemistry of erosion. *J Dent Res* 1967; 46: 1075-1085.
- Liu Y, He L, Mustapha A, Li H, Hu ZQ, Lin M. Antibacterial activities of zinc oxide nanoparticles against *Escherichia coli* O157:H7. *J Appl Microbiol* 2009; 107: 1193-1201.
- Yamamoto O. Influence of particle size on the antibacterial activity of zinc oxide. *Int J Inorg Mater* 2001; 3: 643-646.
- Applerot G, Lipovsky A, Dror R, Perkas N, Nitzan Y, Lubart R, *et al.* Enhanced antibacterial activity of nanocrystalline ZnO due to increased ROS-mediated cell injury. *Adv Funct Mater* 2009; 19: 842-852.
- He G, Pearce EIF, Sissons CH. Inhibitory effect of ZnCl₂ on glycolysis in human oral microbes. *Arch Oral Biol* 2002; 47: 117-129.
- Thanatvarakorn O, Islam MS, Nakashima S, Sadr A, Nikaido T, Tagami J. Effects of zinc fluoride on inhibiting dentin demineralization and collagen degradation in vitro: A comparison of various topical fluoride agents. *Dent Mater J* 2016; 35: 769-775.
- Toledano M, Yamauti M, Osorio E, Osorio R. Zinc-inhibited MMP-mediated collagen degradation after different dentine demineralization procedures. *Caries Res* 2012; 46: 201-207.
- Featherstone JD. Fluoride, remineralization and root caries. *Am J Dent* 1994; 7: 271-274.
- Featherstone JD, Glena R, Shariati M, Shields CP. Dependence of in vitro demineralization of apatite and remineralization of dental enamel on fluoride concentration. *J Dent Res* 1990; 69: 620-625.
- Dige I, Raarup MK, Nyengaard JR, Kilian M, Nyvad B. *Actinomyces naeslundii* in initial dental biofilm formation. *Microbiology* 2009; 155: 2116-2126.
- Nomura R, Morita Y, Matayoshi S, Nakano K. Inhibitory effect of surface pre-reacted glass-ionomer (S-PRG) eluate against adhesion and colonization by *Streptococcus mutans*. *Sci Rep* 2018; 8: 5056.

- 16) Sawair FA, Ryalat S, Shayyab M, Saku T. The unstimulated salivary flow rate in a Jordanian healthy adult population. *J Clin Med Res* 2009; 1: 219-225.
- 17) Bender GR, Sutton SV, Marquis RE. Acid tolerance, proton permeability, membrane ATPase of oral streptococci. *Infect Immun* 1986; 53: 331-338.
- 18) Hamilton IR. Biochemical effects of fluoride on oral bacteria. *J Dent Res* 1990; 69: 660-667.
- 19) Marquis RE. Antimicrobial actions of fluoride for oral bacteria. *Can J Microbiol* 1995; 41: 955-964.
- 20) Nassara HM, Gregory RL. Biofilm sensitivity of seven *Streptococcus mutans* strains to different fluoride levels. *J Oral Microbiol* 2017; 9: 1328265.
- 21) Phan TN, Buckner T, Sheng J, Baldeck JD, Marquis RE. Physiologic actions of zinc related to inhibition of acid and alkali production by oral streptococci in suspensions and biofilms. *Oral Microbiol Immunol* 2004; 19: 31-38.
- 22) Izaguirre-Fernández EJ, Eisenberg AD, Curzon ME. Interactions of zinc with fluoride on growth, glycolysis and survival of *Streptococcus mutans* GS-5. *Caries Res* 1989; 23: 18-25.
- 23) Marinho VC, Higgins JP, Sheiham A, Logan S. Fluoride toothpastes for preventing dental caries in children and adolescents. *Cochrane Database Syst Rev* 2003; 1: 1-103.
- 24) Marinho VC, Worthington HV, Walsh T, Clarkson JE. Fluoride varnishes for preventing dental caries in children and adolescents. *Cochrane Database Syst Rev* 2013; 7: 1-4.
- 25) Horowitz HS, Creighton WE, McClendon BJ. The effect on human dental caries of weekly oral rinsing with a sodium fluoride mouthwash: a final report. *Arch Oral Biol* 1971; 16: 609-616.
- 26) Takatsuka T, Tanaka K, Iijima Y. Inhibition of dentine demineralization by zinc oxide: In vitro and in situ studies. *Dent Mater* 2005; 21: 1170-1177.
- 27) Osorio R, Yamauti M, Osorio E, Ruiz-Requena ME, Pashley DH, Tay FR, *et al.* Zinc reduces collagen degradation in demineralized human dentin explants. *J Dent* 2011; 39: 148-153.
- 28) Katsiki A. Aluminosilicate phosphate cements —a critical review. *Adv Appl Ceram* 2019; 1-13.
- 29) Shah S, Bhaskar V, Venkatraghavan K, Choudhary P, Ganesh M, Trivedi K. Silver diamine fluoride: a review and current applications. *J Adv Oral Res* 2014; 5: 25-35.